Potassium currents underlying the oscillatory response in hair cells of the goldfish sacculus

Izumi Sugihara and Taro Furukawa

Department of Physiology, Tokyo Medical and Dental University School of Medicine, 1-4-45 Yushima, Bunkyo-ku, Tokyo 113, Japan

1. Ionic currents underlying the oscillatory response of membrane potential were studied in oscillatory-type hair cells isolated from the goldfish sacculus with the whole-cell recording method using a patch pipette.

2. Bath application of 4-aminopyridine (4-AP; 10 mM) reversibly produced moderate depolarization of the resting potential along with complete suppression of the oscillatory response. Sustained injection of a small depolarizing current also suppressed the oscillatory response.

3. A 4-AP-sensitive atypical A-type K^+ current which had a high threshold voltage for inactivation ($I_{A(H)}$) was found to be a major outward current underlying the oscillatory response.

4. $I_{A(H)}$ was activated with a time constant of 0·4–10 ms and was inactivated slowly with a time constant of 0·6–2 s. $I_{A(H)}$ activation and inactivation occurred mostly at membrane potentials more positive than −70 mV.

5. There was a clear correlation between activation speed of $I_{A(H)}$ and the frequency of pulse-evoked oscillation. A 'hump'-type response was produced in about one-quarter of the oscillatory-type hair cells.

Based on morphology and their electrical response, goldfish hair cells isolated from the sacculus, the auditory organ of the goldfish (Furukawa & Ishii, 1967), can be divided into oscillatory and spike types (Sugihara & Furukawa, 1989). In response to an injection of depolarizing current, oscillatory hair cells, which are short or ovoid in shape, elicit damped oscillatory changes in membrane potential, not dissimilar to those reported in hair cells of turtle (Crawford & Fettiplace, 1981; Art & Fettiplace, 1987) and chick (Fuchs, Nagai & Evans, 1988) cochleas, frog sacculus (Ashmore, 1983; Lewis & Hudspeth, 1983; Hudspeth & Lewis, 1988*a*, *b*) and other hair cells. However, the ringing in the membrane potential observed in oscillatory goldfish hair cells has been of poor quality, since a maximum of only two or three waves was elicited (Sugihara & Furukawa, 1989), whereas ten or more waves have been seen in the damped oscillatory envelope in turtle cochlear and frog saccular hair cells (Lewis & Hudspeth, 1983; Art & Fettiplace, 1987). Therefore, it is unclear if the electrical oscillations observed in these goldfish hair cells underlie frequency tuning, as has been previously established in, for example, turtle cochlear hair cells.

The present study was aimed at identifying the ionic currents which underlie the damped oscillatory response of goldfish saccular hair cells and at exploring their biophysical properties. It is known that a Ca^{2+}-activated K^+ current ($I_{K(Ca)}$) underlies the oscillatory activity of hair cells in turtle and other animal species mentioned above (Lewis & Hudspeth, 1983; Hudspeth & Lewis, 1988*a*, *b*; Fuchs *et al.* 1988; Fuchs & Evans, 1990; Art, Fettiplace & Wu, 1993). However, the poor quality of the oscillatory responses suggests that different ionic conductances might be involved in goldfish hair cells (Sugihara & Furukawa, 1989; Furukawa & Sugihara, 1990). The present study was facilitated by the use of 4-aminopyridine (4-AP), which almost completely blocks the outward K^+ current in the oscillatory hair cells in the goldfish sacculus. Our results indicate that an atypical A-type K^+ current with a high voltage threshold for inactivation (designated $I_{A(H)}$) is involved in the generation of oscillatory responses in these hair cells.

METHODS

Preparation and experiments

Methods for dissociating single hair cells from the inner ear of goldfish, *Carassius auratus*, and for the set-up of the patch-clamp experiments have been described previously (Sugihara & Furukawa, 1989; Sugihara, 1994). Goldfish were anaesthetized with an intramuscular injection of ketamine hydrochloride (1 mg (g body weight)$^{-1}$). The dorsal skull and the brain were removed to excise the inner ears. Hair cells were isolated from the saccular maculae. All experiments were performed at room

temperature (19–22 °C). When the patch pipette reached the bath, a small constant voltage was applied to the pipette to obtain zero current. After formation of a gigaohm seal (20–100 GΩ), the pipette voltage was shifted by the value of the liquid junctional potential (see below), which should hereafter be absent. The patch membrane was then broken by applying a strong suction to the pipette with the amplifier in voltage-clamp mode at a holding potential of −70 mV. Membrane breakage was heralded by a sudden increase in current transients at the start and end of a small potential step applied to the pipette. The slow transient cancellation circuitry was carefully adjusted in each whole-cell recording by repetitively applying small square pulses under voltage-clamp setting. In voltage-clamp recordings, the series resistance was compensated as much as possible (40–80%). Transient cancellation and series resistance were adjusted several times during recording in each hair cell. The responses were usually observed first in current-clamp mode, then in voltage-clamp mode, and then again in current-clamp mode to observe whether the condition of the cell had remained unchanged. In some of the earlier experiments, only a voltage- or a current-clamp recording was obtained.

The output of the patch-clamp amplifier (EPC7, List Electronic; 10 kHz 3-pole low-pass filter) was recorded either with a PCM data recorder (PR-880, NF Electronic Instruments, Yokohama, Japan) at a sampling interval of 17·4 μs, or directly stored in a computer. The re-played data or the direct output of the amplifier was then passed through a low-pass 4-pole Bessel filter (DT-408, NF Electronic Instruments) at a cut-off frequency of 5 or 1 kHz (−3 dB, 24 dB octave^{-1}), digitized at a sampling period of 50 or 250 μs, for voltage- or current-clamp recording, respectively, stored on the hard disk of a microcomputer (N10, Nippon Data General, Tokyo, or PC-9801RA, NEC, Tokyo) and then printed with a laser printer (PS-801, OKI, Tokyo). For records obtained in voltage-clamp mode, current and command voltage traces are shown at the top and bottom of the figures, respectively. No subtraction for leakage or capacitive currents was applied. To measure the time constant, a single-exponential curve was fitted to the rising phase, inactivation phase or tail decay of the current record using the maximum likelihood method with Simplex minimization (Dempster, 1993). For records obtained in current-clamp mode, potential traces, which were usually averaged from three to six individual traces, are shown at the top, while command current traces are shown at the bottom.

Solutions

The compositions of the pipette and bath solutions are as follows (mM). KCl pipette solution: KCl, 105; Hepes, 5; EGTA, 5; KOH, 20. Potassium citrate pipette solution: potassium citrate, 53; Hepes, 5; EGTA, 5; KOH, 20. Normal Ringer solution: NaCl, 120; KCl, 2; $CaCl_2$, 2; Hepes, 5; NaOH 1·5. TEA Ringer solution: 30 mM tetraethylammonium chloride (TEA) substituted for isomolar NaCl of normal Ringer solution. 4-AP Ringer solution: 10 mM 4-aminopyridine (4-AP) substituted for isomolar NaCl of normal Ringer solution. Ca^{2+}-free Ringer solution: NaCl, 120; KCl, 2; $MgCl_2$, 2; Hepes, 5; NaOH, 1·5. pH was adjusted to 7·2 in all solutions with a small amount of HCl, NaOH or KOH. The liquid junction potentials of KCl and potassium citrate pipette solutions against normal Ringer solution were −5 and −15 mV, respectively. Unless otherwise indicated, normal Ringer solution and KCl pipette solution were used. In some of the earlier experiments, a potassium citrate pipette solution was used. The K^+ concentration in the bath ($[K^+]_o$) was changed by isomolar replacement with Na^+ in reversal potential experiments.

RESULTS

Oscillatory-type hair cells from the rostral and caudal sacculus were studied with both current-clamp and voltage-clamp modes (36 cells), with only current-clamp mode (31 cells) and with only voltage-clamp mode (12 cells).

Suppression of oscillatory responses by 4-AP and prolonged depolarization

As shown in Fig. 1*A a*, short hair cells in the rostral and caudal sacculus responded to depolarizing current pulses with voltage oscillations. When 10 mM 4-AP was applied to the bath, the resting membrane potential was soon shifted from −75 to −50 mV (arrowheads in Fig. 1*A b*) and the oscillatory response was completely abolished, leaving only the passive depolarization with an exponential time course (Fig. 1*A b*). After washing, the resting membrane potential recovered to −78 mV and oscillatory responses reappeared. In all cases of rostral ($n = 3$) and caudal ($n = 7$) oscillatory hair cells, 10 mM 4-AP produced complete blockade of the oscillatory response together with a moderate depolarization of the resting membrane potential.

Injection of steady depolarizing current produced effects very much like those produced by 4-AP. In the control record shown in Fig. 1*Ba*, an 80 pA depolarizing pulse produced oscillatory responses. A steady depolarizing current of 10 pA was then injected, while the response to an identical 80 pA current pulse was monitored every 2 s for a period of 30 s (Fig. 1*B b*). As the injection of steady current began, the resting potential was shifted from a control level of −63 mV to −54 mV (arrow). Although voltage oscillations were initially observed in response to 80 pA pulses (filled arrowhead), they gradually disappeared and changed to a passive response with an exponential-like time course and a larger amplitude (open arrowhead). These results imply a slow inactivation of the outward rectification. Measured at the plateau level, the change in the response corresponded to a conductance decrease to approximately one-quarter of the original value. Phenomena similar to those shown in Fig. 1*B* were seen in all of the cases tested ($n = 3$).

These results indicate that the outward current, which is sensitive to 4-AP and develops slow voltage-dependent inactivation, participates in generating the oscillatory response and in maintaining the resting potential in oscillatory hair cells in the goldfish sacculus.

4-AP blocks outward currents

The effects of 4-AP on ionic currents were examined in the voltage-clamp mode. The transient outward K^+ current (A-current, I_A; Lewis & Hudspeth, 1983; Sugihara & Furukawa, 1989) was distinguishable from other outward currents by the fact that it was activated only when the depolarizing pulse was preceded by a hyperpolarizing prepulse. I_A thus evoked was blocked by 4-AP (90% by 10 mM). However, it is unlikely that the I_A underlies the

oscillatory responses because this current was largely inactivated at the resting potential of the oscillatory hair cells (about −70 mV).

When the membrane potential was held at −70 mV to inactivate I_A, most of the remaining outward current in saccular oscillatory hair cells remained sensitive to 4-AP. In the example shown in Fig. 2*A*, the outward current was almost completely suppressed (to 6%) by 10 mM 4-AP, but recovered after washing. This current can participate in the oscillatory response because it is not inactivated at the holding potential of −70 mV. Its sensitivity to 4-AP suggested that this current belongs to the general A-current class. However, the membrane potential level that produced steady-state inactivation of this current was much more positive than that for typical I_A (see the section below on $I_{A(H)}$ inactivation). Therefore, we referred to this current as an 'atypical A-current with high threshold voltage for inactivation ($I_{A(H)}$)'.

In all of the oscillatory hair cells examined ($n = 10$), the non-I_A component of the outward K^+ current was identified as being mostly $I_{A(H)}$, i.e. it was inhibited by 4-AP (by 90% or more) and showed slow inactivation. Thus, $I_{A(H)}$ seemed to be preferentially expressed in saccular oscillatory hair cells, whereas other K^+ currents, such as 4-AP-insensitive and/or Ca^{2+}-activated ones, were often seen in spike-type saccular hair cells and some lagenar hair cells (e.g. Fig. 5 of Sugihara & Furukawa, 1989).

Effect of TEA and removal of Ca^{2+} on outward currents

TEA (30 mM) partially blocked the outward current in oscillatory hair cells. In the example shown in Fig. 2*Ba*, the outward current was blocked by 46%. The current blocked by TEA was determined by subtracting the remaining current from the control current (Control − TEA in Fig. 2*Ba*). The time course of the blocked component was not dissimilar to that of the remaining current (Fig. 2*Ba*). The effect of TEA was identical in another oscillatory hair cell which had an outward current that was activated more slowly, i.e. partial blockade (by 44%) without a change in the time course (Fig. 2*Bb*), despite the difference in the activation time course of the outward current. In another case (not shown), the outward current was almost completely blocked (90%) by 4-AP, and, after washing out 4-AP, it was partially blocked by TEA (45%). These results suggest that TEA partially blocks $I_{A(H)}$ and that a

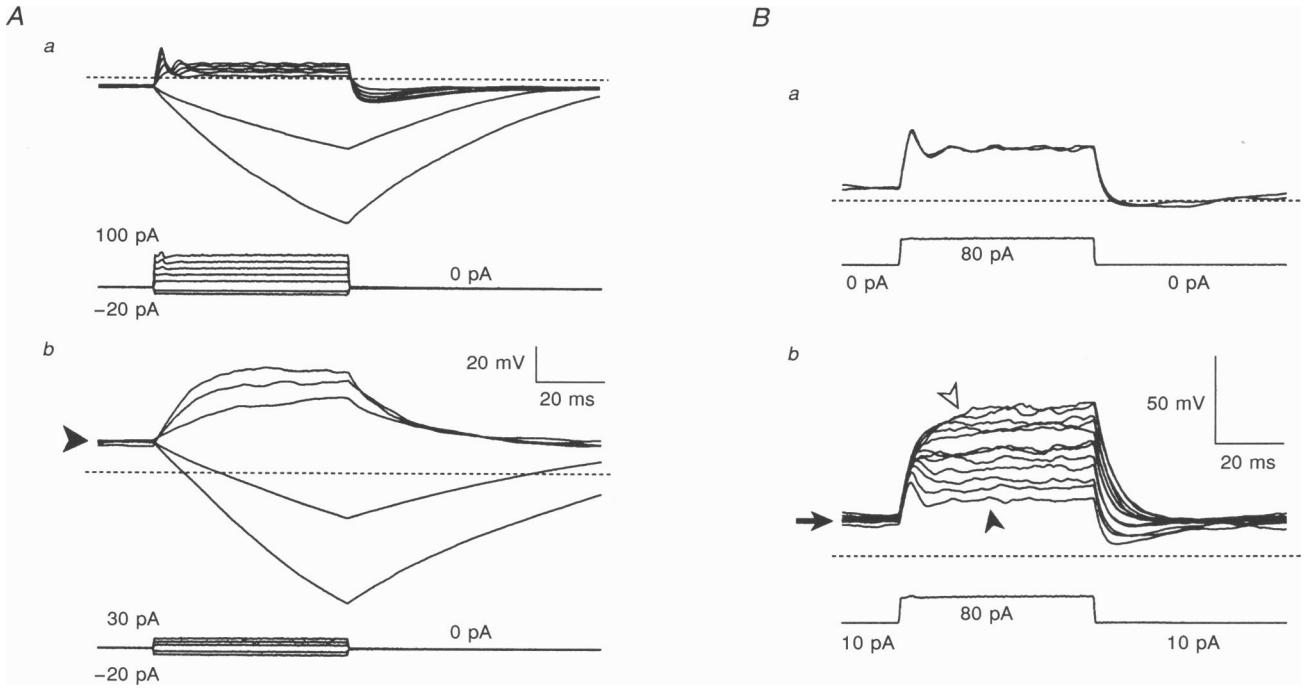

Figure 1. Suppression of oscillatory responses by 4-AP and prolonged depolarization

A, oscillatory responses before (*a*) and after (*b*) 4-AP application. Arrowhead in *b* indicates the resting potential. Records were obtained in current-clamp mode from a short oscillatory hair cell in the rostral sacculus. Traces represent the averages of three to six records. *B*, oscillatory responses evoked by injections of current steps before (*a*) and during the application of a steady depolarizing current of 10 pA (*b*). Test pulses of 80 pA (70 pA plus steady 10 pA in *b*) were given once every 2 s. Traces are not averaged. Arrow in *b* indicates the resting potential. The first and last traces in *b* are indicated by filled and open arrowheads, respectively. Records were obtained in current-clamp mode from a short oscillatory hair cell in the caudal sacculus. Dashed lines indicate −70 mV in *A* and *B*.

significant portion of the outward current in these saccular oscillatory hair cells is $I_{A(H)}$. Similar partial blockade of the outward current by TEA was seen in two other cells. Replacement of the bath solution with Ca^{2+}-free Ringer solution did not suppress the outward current in saccular oscillatory hair cells (Fig. 2*C*). Similar results were obtained in six other cases.

Voltage-dependent activation of $I_{A(H)}$

Figure 3*A* was obtained from a hair cell in which $I_{A(H)}$ represented almost the sole ionic current. The outward current rose quite rapidly and reached a plateau level. After the end of the potential steps, the tail current decayed with a time course of 10–20 ms. The rising phase, except for the initial part, was fitted with single-exponential curves

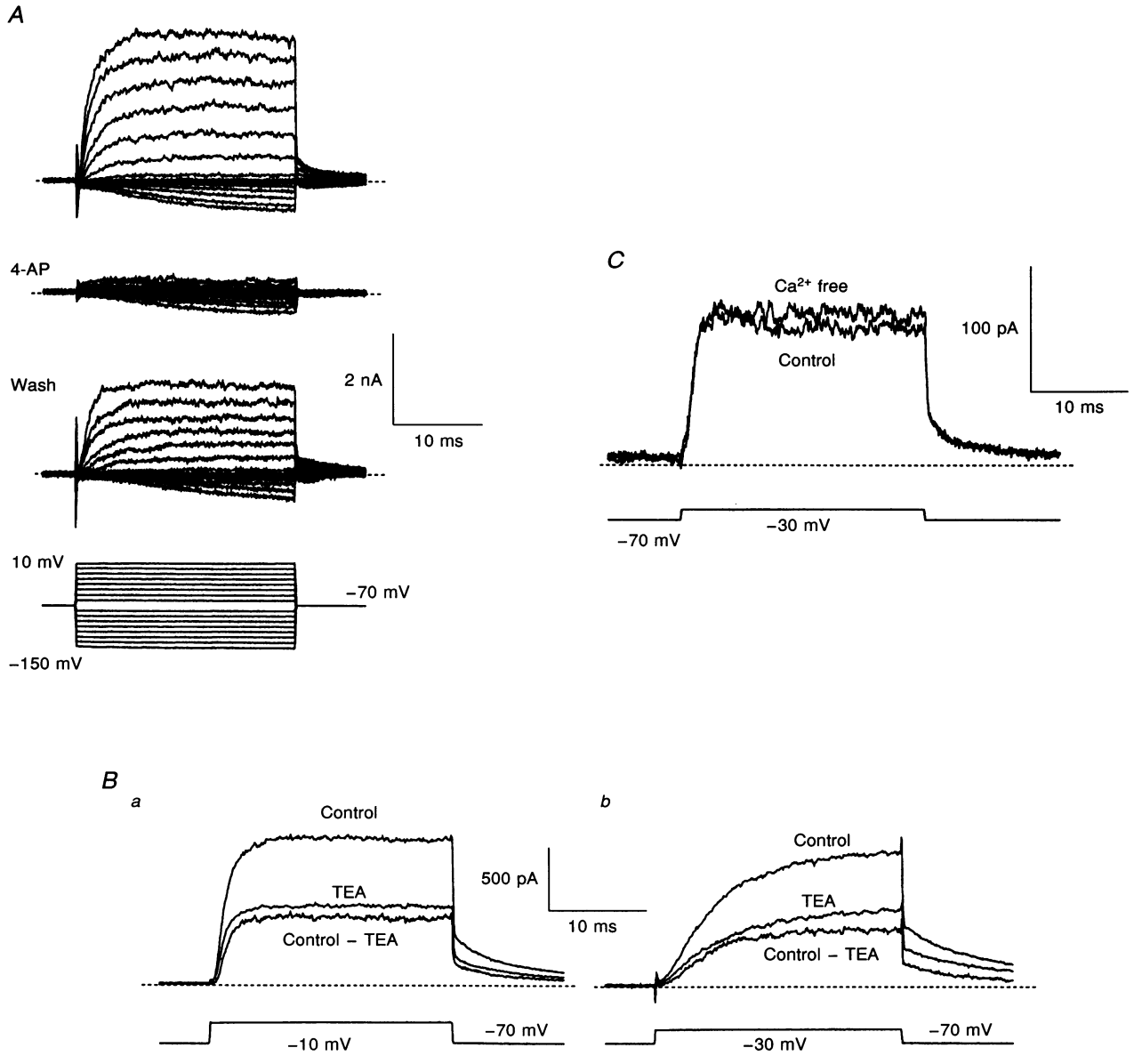

Figure 2. Effects of 4-AP, TEA and Ca^{2+} removal on $I_{A(H)}$ examined in voltage-clamp recordings

A, current before and after 10 mM 4-AP application. Voltage steps up to an amplitude of ± 80 mV were given from a holding potential of −70 mV. Records were obtained from an oscillatory hair cell in the caudal sacculus. *B*, outward current before (Control) and after application of 30 mM TEA recorded in hair cells from the rostral sacculus (*a*) and caudal sacculus (*b*). Amount of current suppressed by TEA, obtained by subtraction (Control − TEA), is also shown. *C*, outward current before and after removal of Ca^{2+} from the bath, recorded in a ovoid hair cell from the rostral sacculus. Dashed lines indicate the zero-current level.

(Fig. 3*B*), the time constants of which were very small (0·47 and 0·89 ms for −30 and −50 mV pulses, respectively). The time constants for the early tail decay (2–3 ms, Fig. 3*D* inset), were greater than those for the rising phase. The steady-state current–voltage (*I–V*) relationship showed activation of the current above −70 mV, and most of the outward current was suppressed by 10 mM 4-AP (Fig. 3*C*). Measured from the initial amplitude of the tail current, the voltage-activation curve showed an S-shaped increase within a potential range from −80 to −10 mV (Fig. 3*D*). This curve was steepest between −70 and −30 mV. Similar voltage-dependent activation was observed in other cases ($n = 46$), although the speed of activation varied (see the section below on oscillation frequency).

Voltage-dependent inactivation of $I_{A(H)}$

$I_{A(H)}$ inactivation was apparent in the responses to long depolarizing pulses (Fig. 4*A*; note the slower time scale). Inactivation proceeded more rapidly for more positive pulses. The time course of this slow inactivation could be fitted with a single exponential function with a time constant (τ) of 600–2200 ms (Fig. 4*A*). This time course of $I_{A(H)}$ inactivation was much slower than that of I_A inactivation (τ: 10–30 ms).

Next, the command pulse to −30 mV was preceded by a prepulse at various levels (duration, 1 s; Fig. 4*B*). Whereas hyperpolarizing prepulses did not produce any marked effect which would indicate the absence of I_A in this cell,

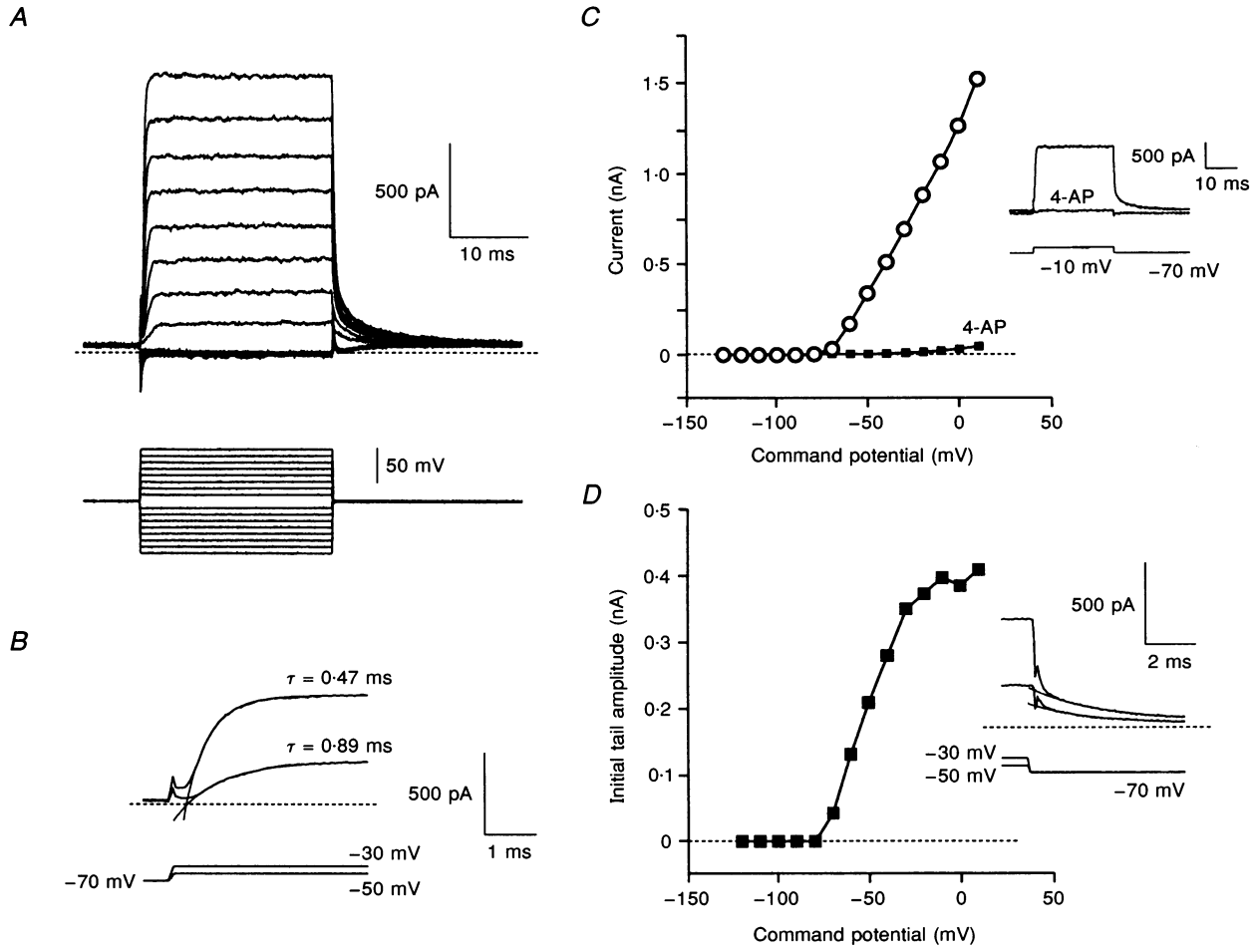

Figure 3. Voltage-dependent activation of $I_{A(H)}$

A, voltage-clamp records obtained by giving pulses (duration, 25 ms) of different amplitude ranging from ±10 to ±80 mV (holding potential, −70 mV). *B*, time constants of activation obtained by fitting the current records with single-exponential curves. *C*, steady-state current–voltage relationship obtained in the traces depicted in *A* (○) and that measured after applying 10 mM 4-AP to the bath (■; inset). *D*, the initial amplitude of the tail current plotted against the command voltage to give the voltage-activation curve for $I_{A(H)}$. Single exponential curves were fitted to the tail current traces (1–12 ms after the offset of the command pulse) to measure the initial amplitude (inset). Data were obtained from an ovoid oscillatory hair cell in the rostral sacculus. Resting potential, −75 mV.

depolarizing prepulses produced various amounts of $I_{A(H)}$ inactivation, which were reflected in the reduced amplitudes of the responses to the command pulse. The relative amplitudes of these responses are plotted against the prepulse potentials in Fig. 4*C* (open circles). As shown, $I_{A(H)}$ inactivation was produced when the prepulse potential was −60 mV or more positive. Relative response amplitudes at the end of a 1 s pulse in Fig. 4*A* are also plotted in Fig. 4*C* (filled squares). They conform fairly well to the result shown with open circles. The range of voltage which led to

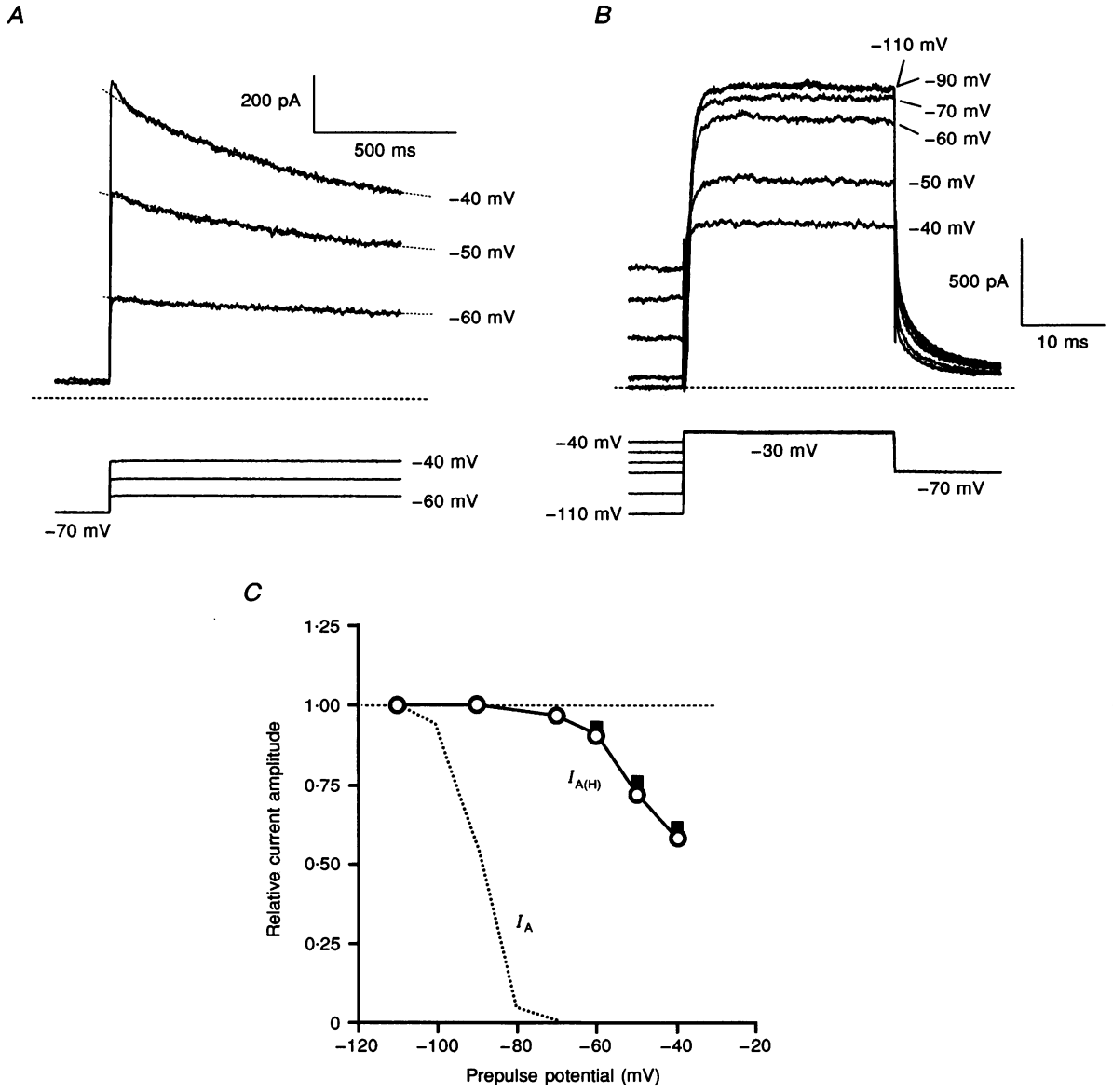

Figure 4. Voltage-dependent inactivation of $I_{A(H)}$

A, current records during 1 s pulses fitted with single-exponential curves. The signal was low-pass-filtered at a frequency of 125 Hz and sampled at 500 Hz. Membrane potential was held at −70 mV before the onset of the pulse. The time constants of fitted single-exponential curves were, from top to bottom, 675, 914 and 2178 ms, and the limiting values were 233, 460 and 591 pA. *B*, current evoked by the command pulse (−30 mV) preceded by a prepulse of 1 s duration. The voltage level during the prepulse is indicated in the figure. Dashed lines in *A* and *B* indicate the zero-current level. *C*, voltage-inactivation curves. ○, relative current amplitude produced by the command pulse preceded by different prepulses, measured in *B*. Reference current was the maximum current elicited when the prepulse was −110 mV. ■, relative current amplitude measured at the end of a 1 s pulse in comparison with the control amplitude at the beginning of the pulse, measured in *A*. The records were obtained from the hair cell used in Fig. 3. The curve for I_A (obtained in a lagenar hair cell which showed large I_A) is also drawn for comparison (dotted line).

inactivation of $I_{A(H)}$ (> −70 mV) was much more positive than that for I_A (−110 to −70 mV, dotted line in Fig. 4*C*). Similar voltage-dependent inactivation was observed in all of the cases examined ($n = 19$).

Reversal potential of $I_{A(H)}$

To determine the ion species that carry $I_{A(H)}$, the reversal potential of the tail current was measured with various external K^+ concentrations ($[K^+]_o$) and a potassium citrate pipette solution ($[K^+]_i$: 179 mM). With $[K^+]_o$ of 5, 10 and 50 mM, the decay of the tail current was most flat at repolarization potentials of −90, −70 and −30 mV, respectively. These values were well fitted by a straight line drawn using Nernst's equation. This result indicates that $I_{A(H)}$ is carried by K^+.

Frequency of pulse-evoked oscillation is correlated with the speed of $I_{A(H)}$ activation

A close correlation has been reported in turtle hair cells between the oscillation frequency and the rising time course of the outward K^+ current (Art & Fettiplace, 1987). In goldfish saccular oscillatory hair cells, the frequency of damped oscillation varies from 30 to 220 Hz (Sugihara & Furukawa, 1989). The time constant of the rising phase of $I_{A(H)}$ ranged from 0·4 to 10·5 ms (with a command pulse of −40 mV) in the present study, i.e. the rate of the rise was occasionally much slower than in the case shown in Fig. 3. The time constant for the tail decay ranged from 2·3 to 11·3 ms (at −70 mV), and the time constant for the slow inactivation ranged from 0·6 to 1·7 s as measured with a command pulse of −30 to −10 mV.

The frequency of these evoked oscillations was compared among hair cells with different speeds of $I_{A(H)}$ activation. Responses of three oscillatory-type hair cells which had different speeds of $I_{A(H)}$ activation are shown in Fig. 5*A*, *B* and *C*. A hair cell in which a high frequency of oscillation was observed (182 Hz at 100 pA; Fig. 5*A a*) showed a high speed of $I_{A(H)}$ activation (τ for rising phase, $\tau_1 = 0{\cdot}47$ ms; τ for tail decay, $\tau_2 = 2{\cdot}7$ ms; Fig. 5*A b*), while another hair cell with a lower oscillation frequency (71 Hz at 80 pA; Fig. 5*B a*) had a lower speed of $I_{A(H)}$ activation ($\tau_1 = 5{\cdot}5$, $\tau_2 = 11{\cdot}3$ ms; Fig. 5*B b*). A hair cell in which the speed of $I_{A(H)}$ activation was even slower ($\tau_1 = 10{\cdot}5$, $\tau_2 = 9{\cdot}3$ ms; Fig. 5*C b*) showed only a 'hump' response (Fig. 5*C a*). However, a smaller $I_{A(H)}$ might also be responsible for the absence of clear oscillations (530 pA in Fig. 5*C b vs.* 680 and 1140 pA in Fig. 5*A b* and *B b*, respectively).

We encountered eighteen 'hump'-type hair cells (Table 1). Both hump-type and typical oscillatory hair cells were short, with a length : width ratio of 1·9 ± 0·7 ($n = 18$) and 2·1 ± 0·8 ($n = 40$), respectively (means ± S.D.), while spike-type hair cells were rather long (length : width ratio,

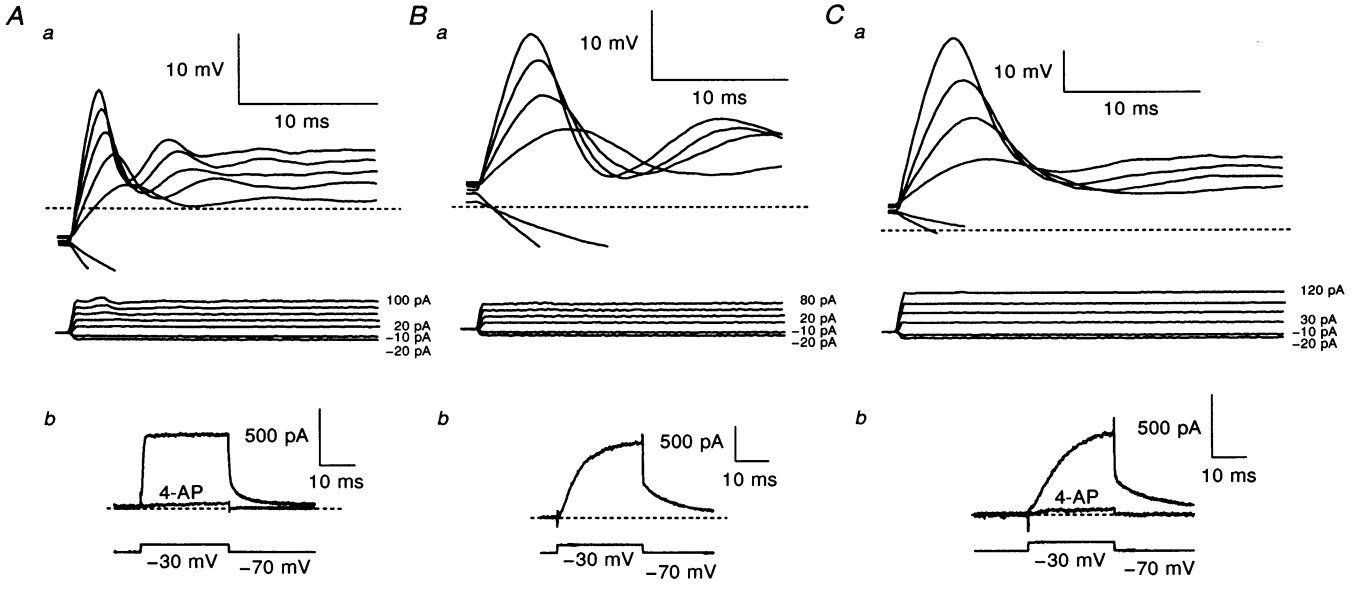

Figure 5. Correlation of the frequency of pulse-evoked oscillation with the speed of activation of $I_{A(H)}$

A, oscillatory responses in a hair cell from the rostral sacculus. *B*, oscillatory responses recorded in another hair cell in the caudal sacculus. *C*, 'hump'-type responses recorded from another hair cell in the caudal sacculus. Initial portion of the potential responses evoked by current injection measured in current-clamp mode (*a*) and current records obtained in voltage-clamp mode (*b*) from the same cells are shown. Each potential record in *A a*, *B a* and *C a* represents the average of three to six records. Dashed lines in current-clamp and voltage-clamp records indicate −70 mV and 0 pA, respectively.

Table 1. Similarity of ion currents among short hair cells which demonstrated oscillatory- or hump-type responses

	Oscillatory-type response			Hump-type response		
Current	I (pA)	n	Percentage of cells	I (pA)	n	Percentage of cells
$I_{A(H)}$	316 ± 324	25	100% (25/25)	239 ± 264	9	100% (9/9)
I_A	104 ± 112	24	79% (19/24)	188 ± 179	8	88% (7/8)
I_h	−97 ± 74	27	81% (22/27)	−146 ± 120	8	100% (8/8)
I_{IR}	0	27	0% (0/27)	0	8	0% (0/8)
I_{Na}	−3 ± 11	23	7% (1/23)	−6 ± 19	7	14% (1/7)

Ionic currents were measured at −30 mV for $I_{A(H)}$, I_A and I_{Na}, and −140 mV for I_h and I_{IR} (results given as means ± S.D.). A total of 67 short hair cells were tested. Of these, the number of hair cells with oscillatory- and hump-type responses was 49 (18 from the rostral sacculus and 31 from the caudal sacculus) and 18 (6 from the rostral sacculus and 12 from the caudal sacculus). Ion currents were measured under voltage-clamp mode in 36 cells.

4·6 ± 1·8, $n = 96$). The hump response seems to correspond to the 'spike' response of toadfish hair cells (Steinacker & Romero, 1992). However, the hump response was distinct from a regenerative spike because the former varied with the intensity of the injected current (Fig. 5*Ca*). In comparison, spike-responses in long hair cells in the caudal sacculus have a self-regenerative all-or-none nature (Sugihara & Furukawa, 1989). Hair cells which showed a clear oscillatory response and those which showed a hump response were similar with regard to the ionic currents involved (Table 1). Thus, outward K^+ currents and hyperpolarization-activated K^+–Na^+ current (I_h; Bader & Bertrand, 1984; Hestrin, 1987; Sugihara & Furukawa, 1989) were observed in both groups of hair cells, whereas inwardly rectifying K^+ current (I_{IR}) was absent. In addition, Na^+ current (I_{Na}) was rarely observed. In fact, I_{IR} and I_{Na} are only expressed in any substantial amount in spike-type hair cells (Sugihara & Furukawa, 1989). Similar 'hump'-shaped responses have been reported in some hair cells in the semicircular canals (Correia, Christensen, Moore & Lang, 1989; Rennie & Ashmore, 1991).

Effects of other currents (I_A and I_h) on the voltage responses

Most oscillatory hair cells (26 of 32) showed I_A together with $I_{A(H)}$ (Table 1). The effects of I_A activation were reflected in a delayed appearance and reduced size of the first peak of oscillation when the resting potential was hyperpolarized (not shown). This was followed by a slowly developing depolarization which reflected a gradual inactivation of I_A.

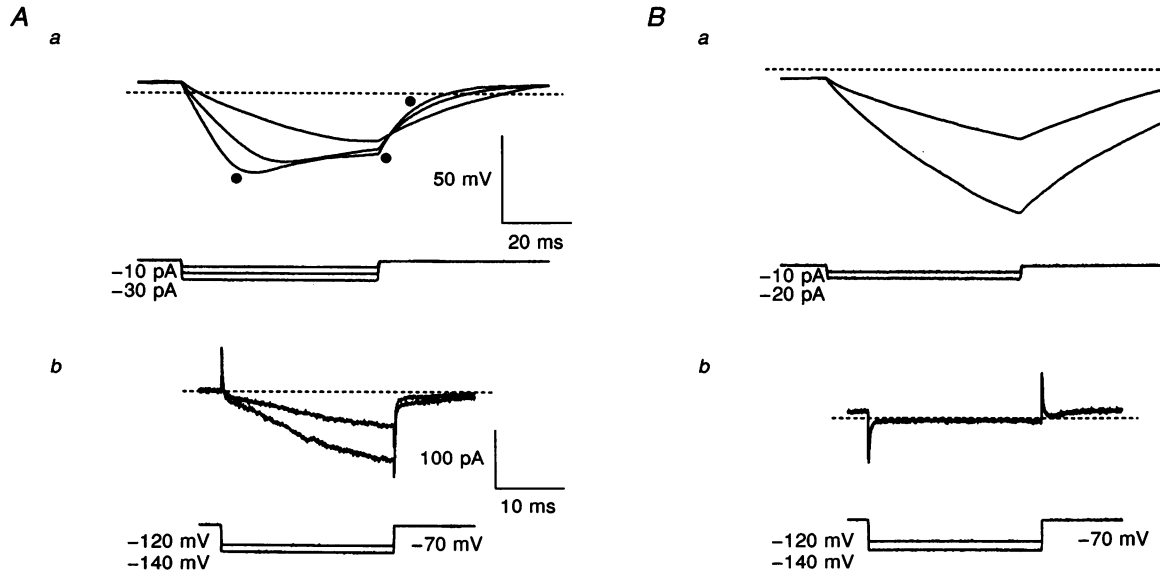

Figure 6. Effect of hyperpolarization-activated potassium–sodium current (I_h) on potential responses

Voltage records (*a*) and current records (*b*) from oscillatory hair cells in the caudal and rostral sacculus which did (*A*) and did not (*B*) have I_h. Response evoked by an injection of −30 pA is marked with filled circles in *A a*. Each potential record in *A a* and *B a* represents the average of three to four records. Dashed lines in current-clamp and voltage-clamp records indicate −70 mV and 0 pA, respectively.

Some oscillatory hair cells have hyperpolarization-activated currents similar to the I_h found in the photoreceptors (Bader & Bertrand, 1984; Hestrin, 1987; Sugihara & Furukawa, 1989). We hereafter refer to the current as 'I_h' in this report because of the similarities of its biophysical properties to those of I_h in other cells (I. Sugihara & T. Furukawa, unpublished data). I_h was seen in thirty of thirty-five oscillatory-type (including hump-type) hair cells (Table 1).

The effect of I_h on changes in membrane potential was examined by comparing the voltage responses between hair cells that did or did not possess I_h (Fig. 6*A* and *B*). When I_h was activated, large hyperpolarizations were inhibited (Fig. 6*A a*). Although I_h began to be activated at potentials more negative than −100 mV, initial hyperpolarization by negative current injections (−20 or −30 pA) could go beyond −100 mV because the activation time course of I_h was slow. However, the membrane potential eventually returned to about −100 mV (Fig. 6*A a*). After the negative current injection, the recovery from hyperpolarization proceeded much more quickly in hair cells that possessed I_h (Fig. 6*A a*) than in those which lacked I_h (Fig. 6*B a*). This was due to the inward tail current of I_h. The I_h tail current could not initiate oscillatory response by itself.

DISCUSSION

$I_{A(H)}$ underlies damped voltage oscillations in goldfish saccular hair cells

In hair cells in which electrical tuning is markedly developed, such as those from the frog sacculus (Lewis & Hudspeth, 1983; Hudspeth & Lewis, 1988*b*) and turtle (Art & Fettiplace, 1987; Art *et al.* 1993) and chicken (Fuchs *et al.* 1988; Fuchs & Evans, 1990) cochleas, $I_{K(Ca)}$ constitutes the predominant pathway for the outwardly rectifying current. However, the results of the present study demonstrated that this does not hold true for oscillatory hair cells of goldfish sacculus. A different K^+ current, i.e. $I_{A(H)}$, underlies the damped voltage oscillations in these hair cells.

The difference in the outward K^+ current may be related to the finding that damped voltage oscillations in goldfish oscillatory hair cells are of a much poorer quality than those reported in frog or turtle hair cells. Quality factor (Q; Crawford & Fettiplace, 1981; Ashmore & Attwell, 1985; Art & Fettiplace, 1987) values as high as 5–10 have been reported in the damped oscillation of the latter group of hair cells, while only much lower values of around 2 could be observed in goldfish oscillatory hair cells (Sugihara & Furukawa, 1989). Authors working on electrical tuning in hair cells unanimously support the idea that the Ca^{2+}-gated K^+ current is much superior to voltage-gated K^+ currents, and have postulated mechanisms for how $I_{K(Ca)}$ could account for the high Q values of oscillation (Ashmore & Attwell, 1985; Hudspeth & Lewis, 1988*b*; Art *et al.* 1993).

As a voltage-gated K^+ current, however, $I_{A(H)}$ seems to have properties suitable for setting up voltage oscillations. First, as shown in Fig. 3*D*, the slope, μ, of the voltage-activation curve (Ashmore & Attwell, 1985), although possibly smaller than that of $I_{K(Ca)}$, is still large, and would favour the generation of voltage oscillations: 0·018 mV^{-1} at membrane potentials between −70 and −30 mV (Fig. 3*D*). When measured by replotting the voltage-activation curves on logarithmic ordinates, the conductance of $I_{A(H)}$ was shown to increase e-fold per 10·3 ± 2·6 mV (mean ± S.D., $n = 4$) between −70 and −50 mV. This value for voltage sensitivity is not greatly different from that for $I_{K(Ca)}$ of frog saccular hair cells: i.e. an e-fold increase per 3 mV (Hudspeth & Lewis, 1988*b*). In addition, $I_{A(H)}$ is only slightly activated at the resting membrane potential and serves to set the resting potential near −70 mV. The value of the fraction of open channels at rest, f_r, obtained from Fig. 3*D* was 0·05 for −75 mV, the resting potential of this hair cell. The smaller the f_r value, the greater the Q value (Ashmore & Attwell, 1985) because depolarization can readily influence $I_{A(H)}$ conductance.

The Q value for goldfish saccular oscillatory hair cells was usually about 2 or less (Sugihara & Furukawa, 1989). These Q values are what would be roughly expected from the properties of $I_{A(H)}$ found in the present study; however, they are slightly greater than 1·46, which was calculated by Ashmore & Attwell (1985) as the maximal Q value that could be produced by a voltage-gated current (for $\mu = 0{\cdot}033$ mV^{-1} and $f_r = 0{\cdot}1$).

With regard to the speed of activation, $I_{A(H)}$ in the oscillatory hair cells of goldfish was often very fast, with a time constant of less than 1 ms (Fig. 3*B*). This speed is comparable to the outward $I_{K(Ca)}$ in the fast oscillatory hair cells of chick cochlea (Fuchs & Evans, 1990), and slightly slower than the fast TEA-sensitive outward K^+ current in the inner hair cells of guinea-pig cochlea (Kros & Crawford, 1990). The speed of activation of the outward current is related more to the oscillation frequency than to Q. In fact, a larger variability was observed in the activation speed of $I_{A(H)}$, and a fast speed of activation of $I_{A(H)}$ tended to be associated with a higher frequency for the damped oscillation (see Fig. 5).

$I_{A(H)}$ in goldfish hair cells compared with K^+ currents in other hair cells

Hair cells in different hair cell organs or in different animal species show different K^+ currents. Several K^+ currents have certain properties similar to those of $I_{A(H)}$. Kros & Crawford (1990) have reported a faster and larger TEA-sensitive current and a slower and smaller 4-AP-sensitive current in guinea-pig cochlear inner hair cells. The $I_{A(H)}$ of goldfish hair cells resembles the latter with regard to the short activation time constant (<10 ms), the lack of fast inactivation, an activation potential range of −60 to −20 mV and sensitivity to 4-AP. However, their 4-AP-

sensitive current does not seem to show slow inactivation (Kros & Crawford, 1990). Slowly inactivating K^+ currents have been reported in some hair cells in semicircular canals. However, they are inactivated substantially near the resting membrane potential (Rennie & Ashmore, 1991; Norris, Ricci, Housley & Guth, 1992) or are more sensitive to TEA than to 4-AP (Lang & Correia, 1989). Thus, none of the ionic currents in hair cells that have been reported thus far are identical to $I_{A(H)}$, although they resemble it in some respects. Actually, $I_{A(H)}$ is not an unusual ionic current, since many similar non-typical 'A-currents' which show slow inactivation at depolarized levels have been reported in various nerve cells (see Rudy, 1988).

$I_{K(Ca)}$ does not play an important role in damped oscillations in oscillatory hair cells in the goldfish sacculus

Ca^{2+}-activated K^+ channels with large conductance (BK channels) have been demonstrated in short (oscillatory-type) as well as long (spike-type) hair cells of the goldfish sacculus (Sugihara, 1994). However, damped voltage oscillations can be attributed to $I_{A(H)}$, whereas the contribution of $I_{K(Ca)}$ is negligible in the present study. BK channels might not be activated during depolarization if Ca^{2+} channels were relatively sparse or were not closely associated with BK channels. In whole-cell voltage-clamp experiments designed to record Ca^{2+} current, either a very small (less than -10 pA at -10 mV, $n = 2$) or undetectable ($n = 10$) current was observed in saccular oscillatory (short) hair cells, whereas spike-type (long) hair cells demonstrated a larger Ca^{2+} current (-10 to -31 pA, $n = 7$). The Ca^{2+} current is also very small in hair cells of pigeon semicircular canals (Lang & Correia, 1989). In contrast, oscillatory hair cells of chick, turtle and frog show large Ca^{2+} currents of -100 to -300 pA (Art & Fettiplace, 1987; Hudspeth & Lewis, 1988*a*; Fuchs, Evans & Murrow, 1990).

Possible contribution of $I_{A(H)}$ in oscillatory hair cells to the phase-locking property of the auditory afferent

According to Fay & Ream (1986) and Cooms & Fay (1987), saccular fibres can be grouped into four categories: (1) untuned, (2) low frequency (LF; best frequency from 120 to 290 Hz), (3) mid-frequency (MF; 330–670 Hz), and (4) high frequency (HF; 790–1770 Hz). We propose that HF and MF fibres receive input from rostral and caudal oscillatory hair cells, respectively, while LF fibres innervate caudal spike-type hair cells (Sugihara & Furukawa, 1989). However, the best frequencies of the MF and HF fibres are much higher than the frequency of the damped oscillation measured on isolated oscillatory hair cells, which is below about 220 Hz. The origin of this large discrepancy has not yet been clarified. The properties of the sound reception and conduction system of the fish might be partially responsible for this difference (see Fig. 6*B* of Furukawa & Ishii, 1967 and the Discussion in Sugihara & Furukawa, 1989). A discrepancy between the frequency of the electrical resonance of the hair cells and the acoustic characteristic frequency of the auditory nerve has also been noted in the alligator lizard and was discussed by Eatock, Saeki & Hutzler (1993).

Based on the low Q values, oscillatory hair cells in the goldfish sacculus do not seem to function as a tool for sharp frequency tuning. This is consistent with a previous finding that single saccular afferent fibres of the goldfish are broadly tuned (Q_{10dB} values, 0·5–0·7; Fay & Ream, 1986). The low Q value indicates that the response area of single oscillatory hair cells spreads widely on either side of the dull peaked optimal frequency region. Furthermore, rapid activation of $I_{A(H)}$ (Fig. 3*B*) would reduce the membrane time constant immediately after stimulus-evoked depolarization, making it possible for the cell to follow each wave of sound up to a higher frequency (see Fig. 12 of Sugihara & Furukawa, 1989). In fact, afferent firings in goldfish are known to remain strictly phase-locked with sound waves of frequencies up to 1000 Hz (Furukawa & Ishii, 1967; Fay, 1978).

Art, J. J. & Fettiplace, R. (1987). Variation of membrane properties in hair cells isolated from the turtle cochlea. *Journal of Physiology* **385**, 207–242.

Art, J. J. & Fettiplace, R. & Wu, Y.-C. (1993). The effects of low calcium on the voltage-dependent conductances involved in tuning of turtle hair cells. *Journal of Physiology* **470**, 109–126.

Ashmore, J. F. (1983). Frequency tuning in a frog vestibular organ. *Nature* **304**, 536–538.

Ashmore, J. F. & Attwell, D. (1985). Models for electrical tuning in hair cells. *Proceedings of the Royal Society* B **226**, 325–344.

Bader, C. R. & Bertrand, D. (1984). Effect of changes in intra- and extracellular sodium on the inward (anomalous) rectification in salamander photoreceptors. *Journal of Physiology* **347**, 611–631.

Cooms, S. & Fay, R. R. (1987). Response dynamics of goldfish saccular fibers: effects of stimulus frequency and intensity on fibers with different tuning, sensitivity, and spontaneous activity. *Journal of Acoustical Society of America* **81**, 1025–1035.

Correia, M. J., Christensen, B. N., Moore, L. E. & Lang, D. G. (1989). Studies of solitary semicircular canal hair cells in the adult pigeon. I. Frequency- and time-domain analysis of active and passive membrane properties. *Journal of Neurophysiology* **62**, 924–934.

Crawford, A. C. & Fettiplace, R. (1981). An electrical tuning mechanism in turtle cochlear hair cells. *Journal of Physiology* **312**, 377–412.

Dempster, J. (1993). *Computer Analysis of Electrophysiological Signals*. Academic Press, London.

Eatock, R. A., Saeki, M. & Hutzler, M. J. (1993). Electrical resonance of isolated hair cells does not account for acoustic tuning in the free-standing region of the alligator lizard's cochlea. *Journal of Neuroscience* **13**, 1767–1783.

Fay, R. R. (1978). Phase-locking in goldfish saccular nerve fibres accounts for frequency discrimination capacities. *Nature* **275**, 320–322.

Fay, R. R. & Ream, T. J. (1986). Acoustic responses and tuning in saccular nerve fibers of the goldfish (*Carassius auratus*). *Journal of Acoustical Society of America* **79**, 1883–1895.

FUCHS, P. A. & EVANS, M. G. (1990). Potassium currents in hair cells isolated from the cochlea of the chick. *Journal of Physiology* **429**, 529–551.

FUCHS, P. A., EVANS, M. G. & MURROW, B. W. (1990). Calcium currents in hair cells isolated from the cochlea of the chick. *Journal of Physiology* **429**, 553–568.

FUCHS, P. A., NAGAI, T. & EVANS, M. G. (1988). Electrical tuning in hair cells isolated from the chick cochlea. *Journal of Neuroscience* **8**, 2460–2467.

FURUKAWA, T. & ISHII, Y. (1967). Neurophysiological studies on hearing in goldfish. *Journal of Neurophysiology* **30**, 1377–1403.

FURUKAWA, T. & SUGIHARA, I. (1990). Multiplicity of ionic currents underlying the oscillatory-type activity of isolated goldfish hair cells. *Neuroscience Research* **12**, S27–38.

HESTRIN, S. (1987). The properties and function of inward rectification in rod photoreceptors of the tiger salamander. *Journal of Physiology* **390**, 319–333.

HUDSPETH, A. J. & LEWIS, R. S. (1988*a*). Kinetic analysis of voltage- and ion-dependent conductances in saccular hair cells of the bull-frog, *Rana catesbeiana*. *Journal of Physiology* **400**, 237–274.

HUDSPETH, A. J. & LEWIS, R. S. (1988*b*). A model for electrical resonance and frequency tuning in saccular hair cells of the bull-frog, *Rana catesbeiana*. *Journal of Physiology* **400**, 275–297.

KROS, C. J. & CRAWFORD, A. C. (1990). Potassium currents in inner hair cells isolated from the guinea-pig cochlea. *Journal of Physiology* **421**, 263–291.

LANG, D. G. & CORREIA, M. J. (1989). Studies of solitary semicircular canal hair cells in the adult pigeon. II. Voltage-dependent ionic conductances. *Journal of Neurophysiology* **62**, 935–945.

LEWIS, R. S. & HUDSPETH, A. J. (1983). Voltage- and ion-dependent conductances in solitary vertebrate hair cells. *Nature* **304**, 538–541.

NORRIS, C. H., RICCI, A. J., HOUSLEY, G. D. & GUTH, P. S. (1992). The inactivating potassium currents of hair cells isolated from the crista ampullaris of the frog. *Journal of Neurophysiology* **68**, 1642–1653.

RENNIE, K. J. & ASHMORE, J. F. (1991). Ionic currents in isolated vestibular hair cells from the guinea-pig crista ampullaris. *Hearing Research* **51**, 279–292.

RUDY, B. (1988). Diversity and ubiquity of K channels. *Neuroscience* **25**, 729–749.

STEINACKER, A. & ROMERO, A. (1992). Voltage-gated potassium current and resonance in the toadfish saccular hair cell. *Brain Research* **574**, 229–236.

SUGIHARA, I. (1994). Calcium-activated potassium channels in goldfish hair cells. *Journal of Physiology* **476**, 373–390.

SUGIHARA, I. & FURUKAWA, T. (1989). Morphological and functional aspects of two different types of hair cells in the goldfish sacculus. *Journal of Neurophysiology* **62**, 1330–1343.

Acknowledgements

This study was supported by Grants-in-Aid for Scientific Research from the Ministry of Education, Science and Culture of Japan. The authors thank Dr E. J. Lang for reading the manuscript.

Received 22 February 1995; accepted 6 June 1995.